



Article citation info:

Zastępa M, The statistical-based diagnosis with usage of acoustic sound decomposition and projected LSTM network of induction motors., *Eksploracja i Niezawodność – Maintenance and Reliability* 2025; 27(3) <http://doi.org/10.17531/ein/205651>

The statistical-based diagnosis with usage of acoustic sound decomposition and projected LSTM network of induction motors

Indexed by:



Marek Zastępa^{a,*}

^a AGH University of Krakow, Faculty of Electrical Engineering, Automatics, Computer Science and Biomedical Engineering, Department of Automatic Control and Robotics, Poland

Highlights

- A novel approach of diagnosing faults of induction motors with acoustic data features.
- The statistical parameters of IMFs are used as a features input.
- A projected LSTM model proposed for motor diagnosis.
- A fast and effective diagnosis of induction motor faults.

Abstract

The use of acoustic signals in the diagnosis of electrical machines allows for non-invasive and rapid diagnostics. The author proposed the novel approach of acoustic diagnosis of single-phase induction motors, which is 98.67% accurate on the test set and allows for fault detection in circa 0.042 s, and 97.33% accurate for 0.021 s long samples similarly. The research includes five classes of faults. In this method, intrinsic mode functions (IMFs) gained from the empirical mode decomposition (EMD) of the motor sound are used to calculate the following statistical parameters: mean, mean square, root mean square, standard deviation, energy, and norm. Next, these parameters are organized from a prepared matrix to a vector of parameters one IMF by one, suitable for neural network input. Such prepared data is then passed to the proposed architecture of the projected LSTM neural network. The training processes were fast - they took only 12 and 13 seconds selectively. The presented novel method is useful for acoustic fault diagnosis of electric motors and could be used for other motors.

Keywords

LSTM, diagnosis, induction motor, empirical mode decomposition, deep learning

This is an open access article under the CC BY license (<https://creativecommons.org/licenses/by/4.0/>)

1. Introduction

Since the invention of semiconductor control devices and their application in induction machine control, the area of application of induction motors significantly increased. Nowadays, they play important roles in industry, power systems, agriculture, services, household appliances, and many others. For example, they are used as an electric drive in car services for car lifting, in workshops for tools drives, or in municipal services to drive water pumps. Three-phase induction motors are also used as an automotive drive. Depending on the context, the machines are used constantly, periodically, or incidentally. In each case,

machine reliability plays an important role for human health and safety. The economic factor is also important. The fast and reliable diagnosis of motors is crucial for real-time monitoring systems or fast diagnosis by motor service in case of malfunction.

In recent years, many types of measurement data have been discussed in literature. With machine learning techniques and appropriate preprocessing methods, they allow us to achieve high accuracies. One of the preprocessing methods is empirical mode decomposition (EMD). This method is mainly used with

(*) Corresponding author.
E-mail addresses:

M. Zastępa (ORCID: 0009-0006-9934-7574) marekzas@agh.edu.pl

Hilbert-Huang transform (HHT). It allows analysis of stationary and non-stationary (or non-linear) natural signals in the time-frequency domain. Therefore, this is one of the significant research areas. The importance of preprocessing has been shown in [1]. The authors applied concatenation of EMD and wavelet packet decomposition to the single-phase current signal. As a result, they distinguished significant differences in energy and RMS of the signal for six levels of tested frequencies. In the article [2], the six-phase permanent magnet synchronous motors with open-circuit faults have been researched. The authors applied the least mean square error (LMS) filter to denoise data, EMD on the current signal data to calculate energy entropy, and normalized average current values of each current phase from IMFs. The SVM classifier with four sub-classifiers accomplished an accuracy of 100% for a healthy state, and 98.3-98.8% for different open-circuit states. The current signal was also researched in [3], where the authors proposed method for feature extraction for broken rotor bar detection with usage of Modified Empirical Mode Decomposition (MEMD) and Adaptive Window Spectral Operation (AWSO). The authors presented fast working original solution for feature extraction. The current signal is obviously not the only type of data used in motor diagnostics. One of the promising areas of research includes the usage of electromagnetic flux, which allows us to classify different types of faults, such as inter-turn short-circuit, broken bars or airgap eccentricity [4]. The article [5] presents four original approaches for thermographic feature extraction: DAMOM (Differences of Arithmetic Mean with Otsu's Method), DAM20HP (Differences of Arithmetic Mean with 20 Highest Peaks), DAMMH (Differences of Arithmetic Mean with Mean of the histogram) and IB (Ignore Binarization) and their usage with Nearest Neighbor (NN) and LSTM networks with grey-scale image inputs. For presented methods, 100% of accuracy has been accomplished in each case. Another approach was presented in [6], in which three states (two faulty and one healthy) of commutator motors have been examined. For this purpose, the author proposed a method called MSAF-RATIO-50-SFC and their variation MSAF-RATIO-50-SFC-EXPANDED. The sum of RSoV was also used. The NN has achieved for the mentioned method selectively: 91.66-93.75% efficiency, the backpropagation neural network (BNN) has achieved selectively: 79.16- 91.66% efficiency, and the linear

discriminant analysis (LDA) achieved: 85.41- 91.66% of efficiency. The vibration data have been also researched in the work [7]. The authors have applied CNN with HHT to diagnose bearing faults on vibration data. The accuracy of CNN with HHT was 98%, and it outperformed CNN with FFT (90%) and CNN with time series (93%) presented in the same paper. In article [8], the authors presented optimized CNN with hyperparameter selection, that achieved 99.8% accuracy on a test set for five classes of bearing faults (including healthy motor). The other area of research in motor faults classification is audio data. In paper [9], the Singular Spectrum Analysis (SSA) with Fast Fourier Transform (FFT) have been used to detect specific components of audio data of Line Start PMSMs with usage of smartphone. The identification of special features, for example in frequency spectrum, is one of the main approaches in classification tasks. The MSAF-20-MULTIEXPANDED was presented in [10] for single-phase induction motor fault detection with the usage of NN, Nearest Mean (NM), and Gaussian Mixture Models (GMM). The best from this research was NM, with a range of accuracy between 89.7-95.3%. The NN and Naive Bayes (NB) were also used in [11] for acoustic motor fault diagnosis. In this article, the SMOFS-NFC method was used, and the range of 89.33%-97.33% of accuracy was achieved for commutator motor fault detection, depending on the variation of the mentioned method. The genetic algorithms are also in use to save the computational resources. The acoustic data have been researched with Acoustic Spectral Imaging (ASI), FFT and CNNs, achieving 93.99-95.62% accuracy [12]. The combination of vibration data with current signals have been researched in [13]. The authors researched performance of KNN, MSVM, RF and ET with feature data obtained from MODWPT decomposition for six classes of bearing states (one healthy). The vibration data combined with magnetic flux have been researched in [14]. The authors proposed CNN with LSTM modules with feature extraction (frequency domain statistical parameters) for six bearing states classification. They achieved 100% accuracy. In [15] presented an approach with the usage of HHT, envelope analysis (EA), and variational mode decomposition (VMD) for feature extraction, and memory space computation genetic algorithm (MSCGA) for feature selection. They were used with SVM, and K-Nearest Neighbor (KNN) classifiers and they achieved 99.4% and 99.14% of

accuracy respectively. Another approach is presented in [16]. The authors focused on bearing fault detection with usage of acoustic data from five microphones. They hired the following machine learning methods: 1D-CNN (accuracy 97.95% without proposed in this paper feature engineering), KNN (accuracy 98.58% with proposed in paper feature engineering, also used for next methods), Decision Tree (98.30%), MLP (95.45%) and SVM (98.86%). Sometimes methods used in other fields are used to diagnose motor faults, like natural language processing. In article [17], the authors proposed method based on Transformer usage with Whale Optimization Algorithm for hyperparameters optimization task. The three-phase current, audio data and vibration data have been collected. The highest accuracy obtained is 99.10% in mentioned paper. Presented so far articles are based on real data for single faulty state at once. Unfortunately, sometimes situations are far more complicated – the data are hard to collect, or handling with composite faults is necessary. To address this issue of insufficient training data, the authors of article [18] proposed a digital twin-driven approach for composite fault diagnosis for subsea production system. This solution allows us to use virtual and real data in the training process, and the diagnosis time is 20 ms. A similar solution was presented in [19], where achieved accuracy is 90% and diagnosed time is 15 ms. In article [20], the digital-twin with cross-validation enhancement has been presented. All these digital-twin methods are promising areas of research, addressing problem of insufficient training dataset.

The CNNs became popular in recent years due to their astonishing performances in many areas. Some of them were already mentioned in the previous paragraph. There are also methods, that are a variation on EMD, like EEMD, CEEMD, or noise eliminated ensemble empirical mode decomposition (NEEEMD) presented in [21] for the scalograms generation. This method used with CNN allowed authors to accomplish 98% accuracy of fault detection on the test set. In [22] authors present multiscale 2D-CNN with attention mechanism and continuous wavelet transform (CWT) analysis of vibration data. The faults of rolling bearings have been examined, and the 98.00% average accuracy has been accomplished. A similar issue was researched in [23] - this paper also presents the 2D-CNN with CWT. For four examined classes the accomplished accuracy was 99.37%. An important issue in artificial

intelligence is the study of “transfer learning” models. Many of them are CNNs. They have already found a lot of applications in many different fields, and the teaching methods used have included both supervised [24] and unsupervised [25] learning. The DenseNet with MobileViT Attention mechanism is one of them, which was researched in [24], where the authors combined four types of DenseNet (Standard DenseNet, MTF-DenseNet, Gdf-Densenet and RP-DenseNet). As a result, the mean accuracy was between 97.35-99.14%, depending on the model. The attention mechanism researched in the mentioned article allowed to reduce diagnosis time by reducing the number of parameters, which is especially important for huge transfer learning models. Głowacz et al. proposed Differences of Word Vectors (DWV) for acoustic feature extraction for transfer learning models: ResNet-18 (100%), DenseNet-201 (100%) and ResNet-50 (100%) [26]. The effectiveness of CNNs in fault detection is undoubtable.

The CNNs are often combined with LSTM networks in fault detection. LSTM networks are a kind of recurrent neural networks with self-loops, that are used for time series data, time steps data, and feature analysis. They seem to be a natural choice for current, vibration, or acoustic data analysis. The PMSM faults were the topic of the research in [27]. In this work, the CNN-LSTM architecture with a hybrid attention mechanism has been proposed for fault detection of 12 classes. The current signal has been used as input data. As the preprocessing method sliding segmentation, Butterworth filter, and FFT were applied. As a result, an accuracy of over 99% has been achieved. Another research [28] focused on PMSM's open-circuit detection with CNN and LSTM networks led to 99.8% accuracy. In [29] the vibration data for the CNN-LSTM network has been applied. The eight classes were examined, and the final accuracies (depending on the accelerometer) ranged from 98.88-99.96%. The Bidirectional LSTM with CNN layers was researched in [30], achieving 99.80% accuracy. Another approach of 1D-LSTM-regulated residual neural network with CNN layer was presented in [31] (100%) accuracy). In [32] the authors proposed FTCNNLSTM (the combination of CNN and LSTM with Attentive Interpretable Tabular Learning) and achieved 96% accuracy for ten classes of bearing faults. The used dataset was CWRU (Case Western Reserve University). Transfer learning CNNs are also combined with LSTMs. The article [33]

presents one of the approaches. The proposed VGG-LSTM achieved 99.53% on test set. Such combination was meant for better handling of long-sequence dependencies with previous feature extraction obtained from CNN transfer learning model. As we can see, the application of LSTMs in fault detection in combination with CNNs is promising.

LSTMs are broadly used in many different fields – including motor fault detection. In [34] authors proposed Highway Bidirectional LSTM with attention mechanism (AHBi-LSTM) for bearing fault detection with usage of vibration data. The overall accuracy of proposed method was 98.23% for six classes, including one normal state. The Highway networks use learnable gating mechanism, which allows to reduce training parameters by controlling flow of information. The deep Bidirectional LSTM with attention mechanism (Abid-LSTM) was also researched in [35]. The input data were multidimensional: the researchers used three-phase current, acoustic data, and vibration data. They achieved an accuracy 99.19%. The focus on complex sensor data is an interesting future research field. The LSTM and GRU networks were researched in [36] with three-phase current signal for PMSMs. For six classes, 98.23% accuracy for LSTM and 98.72% for GRU have been obtained. The acoustic data has been researched with LSTMs too. In [37] authors proposed LSTM-AE with MFCC and DFMT (dynamic feature maximization transformation) in EPS electronic motors' anomaly detection, which achieved 99.2% accuracy for inner and outer rings of bearings state. The application of Huang transform with LSTM has been presented in [38] for audio data of induction motors. The proposed solution achieved an accuracy 96-98% for LSTM network.

The diagnostics of single-phase induction motor faults using acoustic data is an important issue and is still one of the main research problems. The usage of acoustic signals is a universal method – it could be applied to any kind of motor. It is a non-invasive type of measurement, and the microphones are very cheap in comparison to other measurement devices. Even smartphone microphones could be used. The assumption behind the research is the acoustic signals are informative enough to correctly classify the motor state. However, the methods of acoustic diagnosis must satisfy certain requirements. The goals of the research it to obtain reliable and fast working method,

short training time and small required dataset of acoustic data.

The author spotted a suspicious research gap regarding LSTM networks in single-phase induction motor fault detection with usage of acoustic data. Especially with EMD as a preprocessing method. Most of the works are focused on CNNs or combined CNN-LSTM networks. Moreover, most articles do not examine LSTMs with acoustic data. Also, LSTM-P networks have not been researched yet with single-phase induction motors acoustic data. Especially with a set of statistical parameters of IMFs and residuum obtained from EMD. To the best knowledge of the author, there is no similar research work presenting a statistical based method with a presented set of data using EMD and LSTM with projection layers network. The proposed solution provides fast and highly efficient results in single-phase induction motor diagnosis. It is a promising area for further research. In the presented article, the application of the DNNs with projected LSTM layers requires only 12.5 s long samples for each type of fault to train and test the proposed neural network with 98.67% accuracy on 0.042 s long recordings, and similarly, 6.25 s long recordings to get 97.33% accuracy on 0.021 s long samples. Therefore, it also solves the problem of small audio datasets, similarly as transfer learning does. Also, the proposed solution is compact and outperforms many other audio classification methods.

The original and novel contributions of the author are:

- (1) Proposed novel method of classification based on proposed novel architecture of projected LSTM network with the set of statistical parameters calculated from acoustic data with EMD preprocessing method for single-phase induction motor diagnostics,
- (2) high effectiveness, fast work, fast training, fast testing and small requirements of training data of the proposed method. This method addresses the issue of small datasets, similar as transfer learning. Moreover, the proposed neural network is smaller than most transfer learning models.

The rest of the article is organized as follows: Section 2 presents examined induction motors and their faults - the subject of this research. Section 3 provides detailed information about data collection, data preprocessing, and proposed neural network. In section 4 the results of the research have been contained in. The conclusions of the paper are presented in

section 5.

2. The examined induction motors

The majority of produced energy is consumed by electric motors. The induction motors are amongst others, one of the most popular motors due to power electronics controllers, low prices, and good work parameters. We can distinguish mechanical faults and electrical faults. Mechanical damage involves moving parts and material structures, such as damaged bearings, damaged fans, damaged shafts, shaft misalignment, and others. Electrical damage refers to components through which electric current flows. Examples include open circuits in the rotor or stator coil, short circuits in the stator coil, damaged insulation, and others. The other way to divide motor faults can be done by the hierarchical level of fault, such as minor faults (minor bearing damage, small shaft's misalignment), moderate faults (medium bearing damage, medium shaft's misalignment) or severe (broken cage, short-circuit). The faulty machines are also less effective, therefore there is also economic justification for monitoring their states. Some of the faults, like short-circuits in the stator winding, can strongly damage the machine and create a dangerous situation for the user due to the fast increase of temperature in the machine. Other faults may result in louder work, lower torque, an increase in the friction and reduction of the speed or efficiency, and many others. These consequences, like louder work, may also affect human health, and all of these

may lead to a significant reduction in motor life. Therefore, a fast diagnosis is important. The early detected fault should not damage other parts of the machine. It is crucial to detect these kinds of faults before the side effects of faults severely damage the machine. It is estimated that 50% of all faults are bearing faults, and 10% are rotor cage faults [39].

In this research, the following faults have been researched: damaged bearing (moderate fault), broken cage (severe fault), short circuit in starting wiring (severe fault), and short circuit both in starting wiring and work wiring (severe fault), and the healthy motor – 5 classes. The motor with damaged bearing was one machine, the motor with broken cage was second machine, and the motor with short circuit in starting wiring, short circuit both in starting wiring and work wiring and healthy state was third machine (3 states per one machine). Each fault has been artificially made. Each motor has only one fault state (or no-fault) at the time of working, so there are no composite faults. Therefore, the diagnostic task in this case is a multiclass classification problem. The proposed method does not distinguish fault levels - it treats each fault equally. The induction motor data and parameters: Promotor, MY 63 1-4 model, PF = 0.95, speed 1390 rpm, power 0.12 kW, voltage 230 V, mass 3.3 kg. Figure 1. presents all of the induction motors used in the research – (a) with damaged bearing, (b) with broken cage and (c) with both types of short circuit and healthy state.

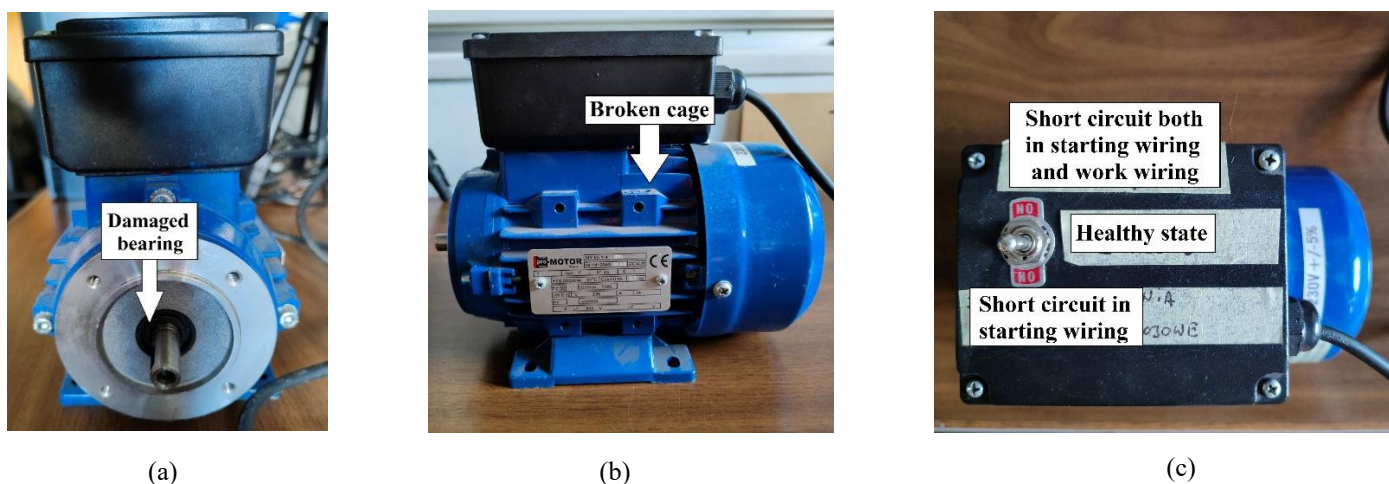


Fig. 1. The examined single-phase induction motor.

3. Materials and methods

3.1. Data collection and preparation

The first author's step of the research was the data collection.

The single-phase induction motor acoustic signals of five classes were collected. For this purpose, a personal computer and Fifine microphone, model K669B (condenser microphone, connectivity technology: wired with USB connection,

sensitivity: -34dB, channels: 1, frequency response: 20-20000 Hz, sampling: 48 kHz / 16 b, impedance: 78 Ohm, cardioid directivity) were used. The microphone was staying on the tripod in front of the induction motor on the concrete floor, at a 0.2 m distance (Fig. 2). The measurements have been performed in a room 5 m × 3 m. The data has been saved in .m4a format. In the second step, the starts and the ends of the recordings have been cut to get rid of the silent and starting/ending parts. This step has been made in the Audacity program. Such prepared data has been split into 1000/48000 = 0.0208 s ≈ 0.021 s long recordings and 2000/48000 = 0.041(6) s ≈ 0.042 s long recordings. The acoustic data were split without any overlapping. No filtering or denoising was used as a preprocessing method in this study, and no normalization has been applied. No dimensionality reduction has been applied. Splitting to samples and all further steps were done with MATLAB 2023b software. The computer parameters: OS: Windows 10 Home, processor: Intel(R) Core(TM) i7-9750H CPU, RAM: 12 GB. In further steps, 300 samples of each class have been used (1500 samples in total).

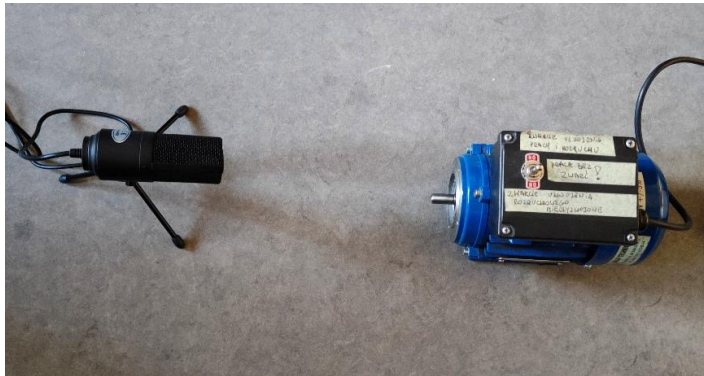


Fig. 2. The measurement setup.

3.2. Empirical mode decomposition, statistical parameters, data set preparation

The EMD (and its variations) became one of the research areas in recent years in motor fault diagnosis [1, 2, 7, 15]. The EMD algorithm generates an unknown number of time-domain functions called intrinsic mode functions (IMFs). Each IMF represents one of the signal intrinsic mode oscillators. Among the identified oscillators we can distinguish oscillators without zero crossing, which are eliminated via a process called sifting, and they do not take part in further analysis. The IMF functions allow for fully and correctly reconstructing signals. These functions must fulfill the following requirements: zero-mean

value and an equal number of maximum values and cross-zero values or their differ by at most one. The algorithm with steps is presented in detail in [40, 41]. The EMD could be applied both to stationary and non-stationary signals, therefore it is widely used. The motor signals (without noise and in the normal work state of the machine, not during the start) are stationary in most cases. The EMD is mainly used with Hilbert spectral analysis, which together form the Hilbert-Huang transform. This useful mathematical tool found already a lot of applications: in physics [42], neuroscience [43], power system fault diagnosis [44], seismic studies [45, 46], and many others. The HHT, and EMD also on their own, allow to analyze data in the time-frequency domain. However, EMD provides IMFs and residual, which are still in the time domain. This can be shown by the formula (1) (from [32]).

$$x(t) = \sum_n x_n(t) + r(t) \quad (1)$$

where: $x(t)$ is a signal, $x_n(t)$ is an n -th IMF, and $r(t)$ is a residual. Therefore, it is justified to use statistical parameters of signal typical for time domain analysis. The set of parameters presented below refers to the changes in acoustic signal depending on the type of motor class. In this research, following parameters have been applied: mean \bar{x} (2), mean square value x_{MS} (3), root mean square x_{RMS} (4), standard deviation σ (5), energy E (6) and norm $\|x\|$ (7), where: x_n n -th sample of signal, N – number of samples.

$$\bar{x} = \frac{1}{N} \sum_{n=0}^{N-1} x_n \quad (2)$$

$$x_{MS} = \frac{1}{N} \sum_{n=0}^{N-1} x_n^2 \quad (3)$$

$$x_{RMS} = \sqrt{\frac{1}{N} \sum_{n=0}^{N-1} x_n^2} \quad (4)$$

$$\sigma = \sqrt{\frac{1}{N} \sum_{n=0}^{N-1} |x_n - \bar{x}|^2} \quad (5)$$

$$E = \sum_{n=0}^{N-1} |x_n|^2 \quad (6)$$

$$\|x\| = \sqrt{\sum_{n=0}^{N-1} |x_n|^2} \quad (7)$$

For each IMF a mentioned set of parameters is calculated.

They are organized into the matrix as follows: the row of parameters, and columns of IMFs. Next, the training set, validation set, and test set have been divided in proportion 0.70:0.15:0.15 respectively. The dataset was balanced. Each class was present in number: 210 in the training set (1050 in total), 45 in the test set (225 in total), and 45 in the validation set (225 in total). The data have been converted into the vector,

adequate for the neural network's feature input. Supervised learning has been applied. There was no data leaking between datasets, and the entire dataset was randomly shuffled before splitting into training, validation and test set. No augmentation has been performed. The flowchart of the entire process is presented in Fig. 3.

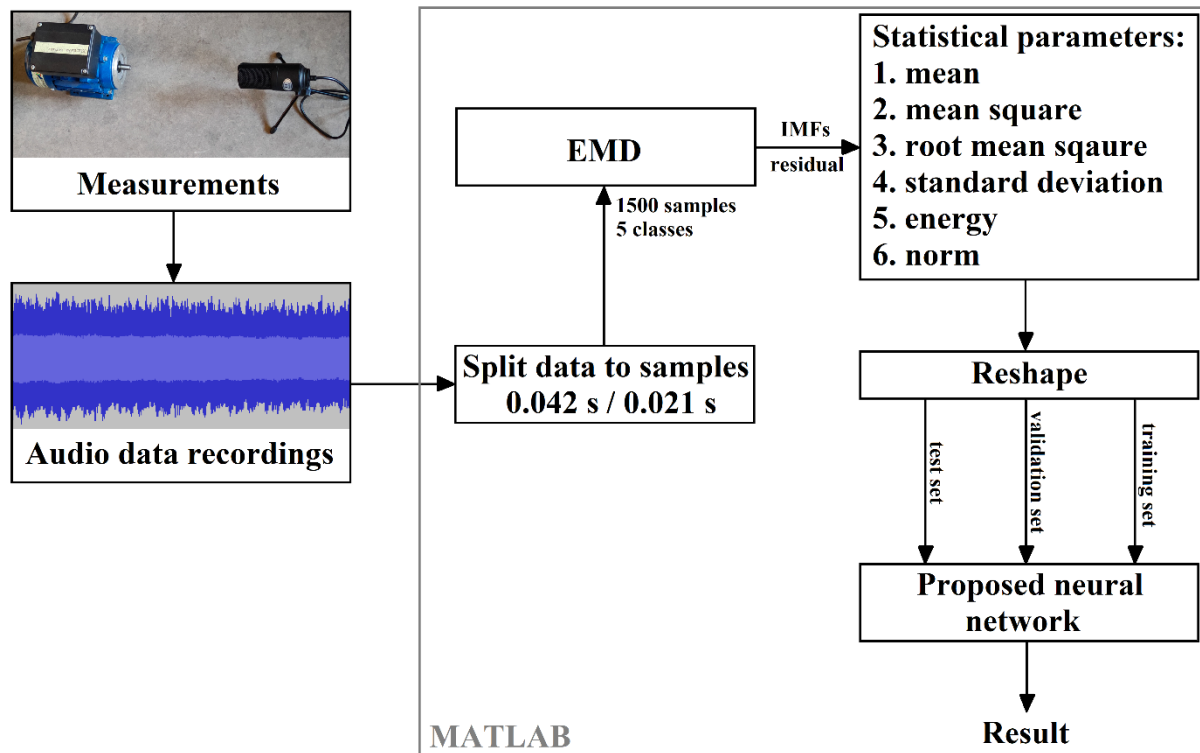


Fig. 3. The flowchart of the proposed method.

3.3. Projected LSTM Deep Neural Network

Long short-term memory (LSTM) has been invented to address the problem of numerical instability of the recurrent neural networks' training (vanishing gradient) and became, as did CNN, one of the most popular neural networks due to their high performances. The single neuron consists of the cell, input gate, output gate, and forget gate, where the cell is responsible for remembering and gates are responsible for data flow by assigning 0 or 1 weight for the particular state. The LSTM is well described in [47]. However, there is the possibility to improve LSTM networks by adding the projection layer. The projection layer is responsible for simple, additional matrix multiplication on the output of the LSTM layer by a new matrix called the projector matrix. This linear operation on the matrices reduces the number of learnable parameters. As a result, the numerical complexity of the neural network decreases and the

accuracy may increase, depending on the task. Also, the training process is faster. The projector matrix is a learnable part of the layer [48,49]. The author proposed DAGNetwork with LSTM projection layers. The parameters of the proposed network are presented in Tab. 1., and their graph is presented in Fig. 4.

The feature input layer was applied according to the characteristics of the dataset. We can consider the presented dataset as ordered sub-sequences of features. This layer also provides data normalization appropriate for this task. The first row in Table 1 shows that the input of the neural network depends on the number of IMFs. This solution allows us to automatically adjust the neural network's input to the changed settings (the number of IFMs, for example). For this kind of data, hiring the batch normalization layer provides an increased speed of training and better accuracy. This layer also increases the stability of the training process. The activation function in every

case is ReLU. The dropout layer is set to 0.4 value – this value was determined experimentally as the best and as a result, significantly increased the performance of both models. On the output of the neural network, there are fully connected layer with outputs equal to number of classes, a softmax layer (recommended for multiclass classification tasks), and a classification output layer.

Table 1. Parameters of the proposed neural network.

Name	Type of layer	Parameters
Feature Input	featureInput	$S = (N_{IMF} + 1) \cdot N_{SP}$
LSTM-P 1	lstmProjectedLayer	HU = 108, OPS = 68, IPS = 108
BatchNorm 1	batchNormalizationLayer	-
ReLU 1	reluLayer	-
LSTM-P 2	lstmProjectedLayer	HU = 108, OPS = 68, IPS = 108
BatchNorm 2	batchNormalizationLayer	-
ReLU 2	reluLayer	-
LSTM-P 3	lstmProjectedLayer	HU = 216, OPS = 68, IPS = 108
BatchNorm 3	batchNormalizationLayer	-
ReLU 3	reluLayer	-
FC 1	fullyConnectedLayer	OS = 108
BatchNorm 4	batchNormalizationLayer	-
ReLU 4	reluLayer	-
Concatenation	concatenationLayer	3 inputs
Dropout	dropoutLayer	0.4
FC 2	fullyConnectedLayer	Number of classes = 5
Softmax	softmaxLayer	-
ClassOutput	classificationOutput	-

where: S - input size, N_{IMF} - number of IMFs, N_{SP} - number of statistical parameters, HU – number of hidden units, OPS – output projector size, IPS - input projector size, OS – output size.

For both models, the following training options have been set: initial learning rate = 0.006, mini-batch size = 44, max epochs = 26, validation frequency = 44, execution environment = CPU, optimizer - SGDM. Total number of learnable parameters: 370900. The MATLAB environment with Deep Learning Toolbox was used.

The presented approach integrates LSTM networks with EMD preprocessing method for acoustic data classification task. As was already meant in section 3.2., we can obtain with EMD oscillators, which are time-domain functions. Therefore, we can calculate their statistical parameters. The EMD allows us to obtain a lot of information from the signal. LSTM networks are famous due to their excellent performance in long sequences

handling. The presented approach allows us to determine dependencies between statistical parameters of each oscillator and residual for each state of the motor with LSTM. This solution constitutes a noise reduction and identification process. The determination of oscillators allows us to analyze shorter time samples for chosen number of functions, which results in faster work of neural network or possible real-time solution. Also, high accuracy has been achieved. This approach addresses the problems of small training dataset, fast working, fast training process and robust diagnosis of single-phase induction motor diagnosis.

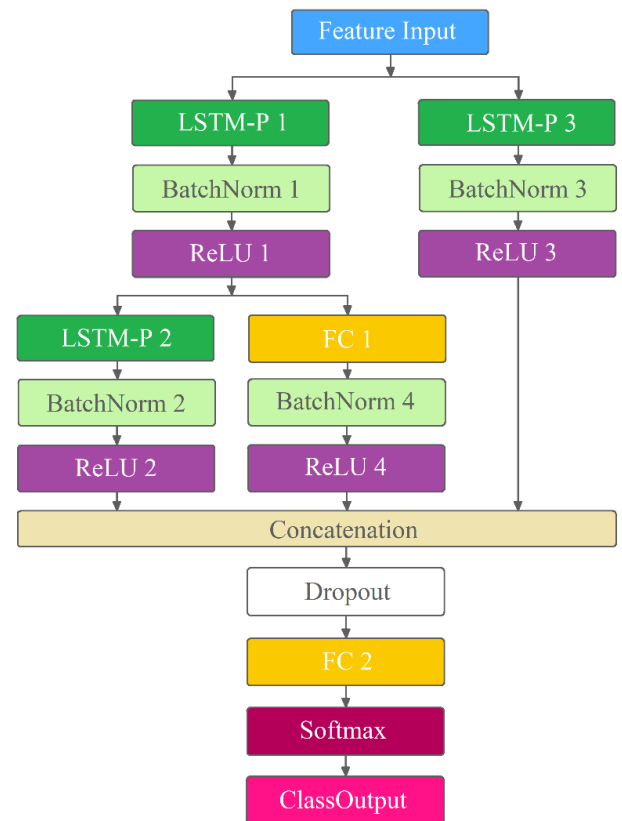


Fig. 4. The graph of the proposed LSTM-P network.

4. Results

The research was conducted for five classes of induction motors: four faults (damaged bearing, broken cage, short circuit in starting wiring, and short circuit both in starting wiring and work wiring) and one without faults. The labels have been conducted by the author for entire dataset. The induction motors were powered by a 230 V / 50 Hz voltage source. The author collected acoustic data, prepared data for further processing, proposed the novel method and the neural network's architecture, carried out the calculations and the experiment, and performed the evaluation of the obtained models.

One of the most important issues in this research was to find the best number of IMFs for neural network training. The accuracy of the networks on the test set depends on the number of IMFs. By trial-and-error method, the number of IMFs for 0.042 s samples is optimal in 4 plus residual, and 6 plus residual

for 0.021 s samples. For both cases, Fig. 5. and Fig. 6. present IMFs and residual for healthy induction motor of 0.042 s and 0.021 s samples respectively. The training process took 13 s for 0.021 s samples and 12 s for 0.042 s samples.

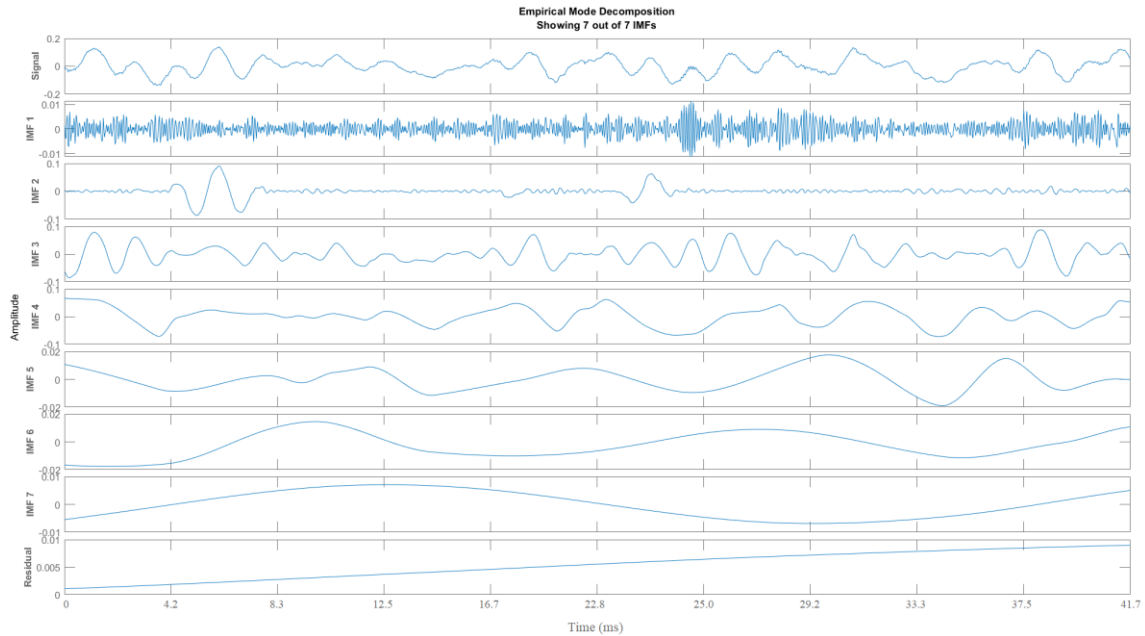


Fig. 5. The presentation of IMFs and residual for 0.042 s sample of healthy motor.

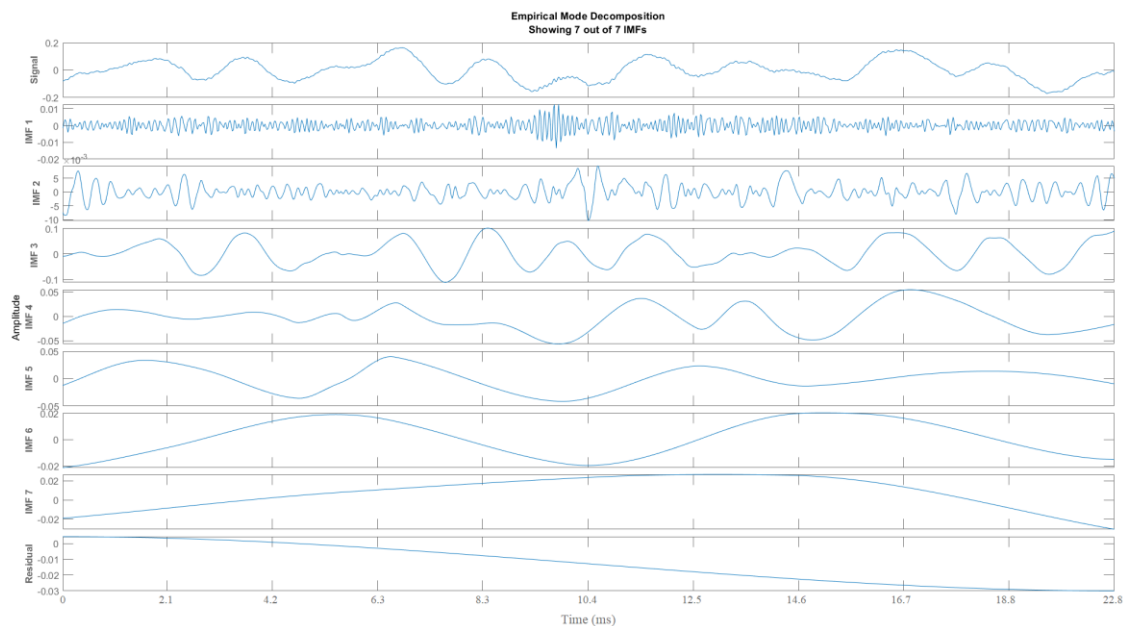


Fig. 6. The presentation of IMFs and residual for 0.021 s sample of healthy motor.

The confusion matrices are shown in Fig. 7 a) and b) for 0.042 s and 0.021 s samples respectively. The shorts of classes are as follows: F1 – no faults, F2 – damaged bearing, F3 - short circuit in starting wiring, F4 - short circuit both in starting wiring and work wiring, F5 - broken cage. In both presented

cases noteworthy is that the main misclassifications are between F3 and F4 classes, so two types of short-circuit, which are similar severe faults. There is no misclassification between F1 and F3 or F4, therefore there are no seriously dangerous errors. The misclassification with fault F1 occurred with a damaged

bearing. For (a) there is 1 misclassification between classes F1 and F2 - false healthy state (the true is damaged bearing, which is moderate fault), and for (b) it is false damaged bearing classification. Due to the balanced dataset, the metric used to evaluate the models is accuracy (8), where A – accuracy. The

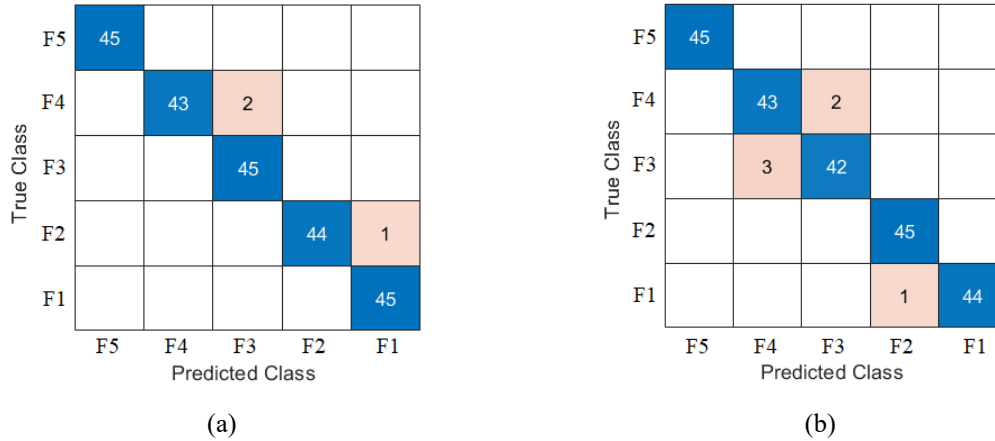


Fig. 7. The confusion matrices for (a) 0.042 s samples and (b) 0.021 s samples.

$$A = \frac{\text{Correct classifications}}{\text{All classifications}} \cdot 100\% \quad (8)$$

The training process took only 12 s and 13 s respectively for 0.042 s samples and 0.021 s samples; therefore, the training process is also very fast. The entire dataset contains 1500 samples, 300 of each class. That means 12.5 s recordings of each class for 0.042 s samples are sufficient for the neural network's training and evaluation. Similarly, 6.25 s recordings of each class for 0.021 s samples are sufficient. This method also addresses the problem of small datasets. Furthermore, the time of diagnosis process from .wav file loading to end of classification process has been measured and presented below. For 0.042 s recordings it took 0.008 s on average for the entire dataset (11.957 s / 1500 samples). For 0.021 s recordings it took 0.007 s on average for the entire dataset (10.954 s / 1500 samples).

5. Discussion

The electrical motor faults classification have been widely researched within different types of data: current signal, vibrations, thermographic, magnetic flux and acoustic. The limitations of acoustic signal classification are weather conditions (e.g. storms), other working machines and appliances generating sounds, human speech and so on. As in other solutions, the conditions of measurements should be identified and carefully checked.

Table 2 presents comparison of proposed method with

accuracy achieved for test set for 2000 probes per sample (0.042 s) is 98.67%, and for 1000 probes per sample (0.021 s) is 97.33%. For the validation set, the accuracies were equal 95.56% and 94.67% respectively.

findings from other articles. Some information about the entire process has not been provided in some of these articles, therefore appropriate information has been added to the table. Also, special attention should be paid when comparing the following metrics: training time and testing time - their values will depend on several factors, including the hardware on which the calculations were performed.

Based on the information presented in Table 2, we can clearly see the superiority of the proposed method in terms of training time, testing time and dataset size. Also, the sample length used in research is one of the shortest ones. The accuracy on test set is outperforming most LSTM-based approaches – only GRU presented in [36] performed slightly better for similar number of classes. Also, in [35] the 3D Chaotic MPIO ABid-LSTM have higher accuracy, but it also has higher time metrics. The method from [8] using vibration data allows to achieve 99.8% accuracy with similar length samples, 0.02 s, but longer training time (1256 s), larger dataset – 1500 samples per each class, less than 45 s per each class (in this research, the entire dataset for all five classes had similar size) and longer testing time, circa 0.030 s. However, presented in this article accuracy is still lower than for multidimensional data, e.g. in [35] - 99.19%. In research [37] accuracy was slightly higher (99.2%), but number of classes was only two – normal work and anomaly.

Therefore, the integration of EMD and LSTM networks provides promising results. For further research, improving

time diagnosis, shortening sample length, increasing accuracy and providing more robust solutions are the most important goals.

Table 2. Comparison of the proposed method with other methods in the literature.

Reference	Training time (s)	Testing time (s)	Accuracy on test set (%)	Number of classes	Dataset size (s)	Sample length
CNN [8]	1256	0.03	99.8	13	585	0.02
LSTM [34]	NP	NP	89.57	7	770	NP
Bi-LSTM [34]	NP	NP	91.60	7	770	NP
Bi-LSTM+Highway [34]	NP	NP	93.44	7	770	NP
Bi-LSTM+Attention [34]	NP	NP	95.41	7	770	NP
AHBi-LSTM [34]	NP	NP	98.23	7	770	NP
LSTM [35]	558	0.034	61.45	4	NP	NP
Bid-LSTM [35]	882	0.041	74.25	4	NP	NP
PIO-LSTM [35]	3684	0.045	90.14	4	NP	NP
HHO-Bid-LSTM [35]	4362	0.041	93.57	4	NP	NP
3D Chaotic MPIO ABid-LSTM [35]	3894	0.041	99.19	4	NP	NP
Transformer [35]	690	0.030	94.17	4	NP	NP
LSTM [36]	8240	NP	98.23	6	2304*	0.1
GRU [36]	5100	NP	98.72	6	2304*	0.1
LSTM [38]	NP	1.8	98	8	NP	NP
Proposed: 42 ms	13	0.008	98.67	5	62.5	0.042
21 ms	12	0.007	97.33		31.25	0.021

NP – not provided; * in total; for each scenario per each class, it was 48 s

6. Conclusions

The proposed novel method of statistical-based diagnosis of induction motors with EMD and LSTM-P network performed very well. It works very fast, and the training process is very short. The optimization of the neural network with dropout layer, selection of appropriate hyperparameters, selection of the best normalization layers, and activation functions provided higher accuracies. The hiring of the EMD and statistical parameters provided good performance. The statistical parameters have been selected very well. LSTM-P networks can be successfully used for this kind of task and should be considered in further research. All of this allows this method to be used in early fault detection systems, and real-time applications or to be used as an independent system or auxiliary sub-system of fault detection. Combination of audio data-based diagnosis sub-system with other types, e.g. vibration data, flux data and current data. Specifically, the real-time application in continuous motor diagnosis seems to be promising due to the short time of required samples, relatively simple preprocessing and fast work of proposed neural network. This method should be used

successfully for other types of electrical motors, like other asynchronous motors, synchronous motors, commutator motors, DC motors and others. Therefore, it should be useful for diagnosis of electrical tools' motors, tram motors, train motors and many others.

The limitation of this method is the necessity to experimentally select the optimal number of IMFs. The number of IMFs affects the final accuracy. The small sample size of training set for each class required for proposed solution is a significant advantage and is within an acceptable range for presented task, but on the other hand it may affect the generalizability of the findings. Therefore, further research should be focused on larger datasets and datasets with higher number of classes. The generalizability of the model and method should be examined. Also, another set of statistical parameters should be investigated. Other types of motors and a bigger number of fault classes also should be tested. Another area of further research should include multi-label (or multi-fault, in other words) diagnosis. Also, multisensory and multidimensional data should be researched, such as combination of current data, vibration data, and acoustic data.

References

1. Refaat SS, Al-Shemmary A, Abdulmawjood K, Kameli SM, Abuelrub A. Static Eccentricity Fault Analysis in Three-Phase Induction Motors Using Current Signal. 2023 IEEE International Conference on Metrology for eXtended Reality, Artificial Intelligence and Neural Engineering (MetroXRINE); 25-27 October 2023; Milano, Italy. IEEE; 2023 <https://doi.org/10.1109/metroxraine58569.2023.10405822>
2. Wu Y, Zhang Z, Li Y, Sun Q. Open-Circuit Fault Diagnosis of Six-Phase Permanent Magnet Synchronous Motor Drive System Based on Empirical Mode Decomposition Energy Entropy. IEEE Access 2021; 9: 91137-91147, doi:10.1109/ACCESS.2021.3090814
3. Arifin MS, Wang W, Uddin MN. A Modified EMD Technique for Broken Rotor Bar Fault Detection in Induction Machines. Sensors 2024; 24(16), <https://doi.org/10.3390/s24165186>
4. Mazaheri-Tehrani E, Faiz J. Airgap and stray magnetic flux monitoring techniques for fault diagnosis of electrical machines: An overview. IET Electr Power Appl. 2021; 16(3) 277-299, doi: <https://doi.org/10.1049/elp2.12157>
5. Głowacz A. Thermographic fault diagnosis of electrical faults of commutator and induction motors. Eng Appl Artif Intell. 2023; 121 105962, <https://doi.org/10.1016/j.engappai.2023.105962>
6. Głowacz A, Głowacz W. Vibration-Based Fault Diagnosis of Commutator Motor. Shock and Vibration 2018; 2018: 1-10, <https://doi.org/10.1155/2018/7460419>
7. Du D, Zhang J, Fang Y, Tian J. Motor Bearing Fault Diagnosis based on Hilbert-Huang transform and Convolutional Neural Networks. 2022 IEEE Transportation Electrification Conference and Expo, Asia-Pacific (ITEC Asia-Pacific); 2022; Haining, China, 1-5, IEEE; 2022, <https://doi.org/10.1109/ITECAsia-Pacific56316.2022.9941910>
8. Skowron M, Frankiewicz O, Jarosz JJ, Wolkiewicz M, Dybkowski M, Weisse S et al. Detection and Classification of Rolling Bearing Defects Using Direct Signal Processing with Deep Convolutional Neural Network. Electronics 2024; 13(9), <https://doi.org/10.3390/electronics13091722>
9. Maraaba LS, Memon AM, Abido MA, AlHems LM. An efficient acoustic-based diagnosis of inter-turn fault in interior mount LSPMSM. Appl Acoust. 2021; 173 107661, <https://doi.org/10.1016/j.apacoust.2020.107661>
10. Głowacz A, Głowacz W, Głowacz Z, Kozik J. Early fault diagnosis of bearing and stator faults of the single-phase induction motor using acoustic signals. Measurement 2018; 113: 1-9, <https://doi.org/10.1016/j.measurement.2017.08.036>
11. Głowacz A, Tadeusiewicz R, Legutko S, Caesarendra W, Irfan M, Liu H et al. Fault diagnosis of angle grinders and electric impact drills using acoustic signals. Appl Acoust. 2021; 179 108070, <https://doi.org/10.1016/j.apacoust.2021.108070>.
12. Hasan Md J, Islam MMM, Kim J-M. Acoustic spectral imaging and transfer learning for reliable bearing fault diagnosis under variable speed conditions. Measurement 2019; 138: 620-631, <https://doi.org/10.1016/j.measurement.2019.02.075>.
13. Afia A, Gougam F, Touzout W, Rahmoune C, Ouelmokhtar H, Benazzouz D. Spectral proper orthogonal decomposition and machine learning algorithms for bearing fault diagnosis. J Braz Soc Mech Sci Eng. 2023; 45 550, <https://doi.org/10.1007/s40430-023-04451-z>
14. Rajabioun R, Afshar M, Atan Ö, Mete M, Akin B. Classification of Distributed Bearing Faults Using a Novel Sensory Board and Deep Learning Networks With Hybrid Inputs. IEEE Transactions on Energy Conversion 2024; 39(2): 963-973, doi: 10.1109/TEC.2023.3338447
15. Lee C-Y, Le T-A, Hung C-L. A Feature Selection Approach Based on Memory Space Computation Genetic Algorithm Applied in Bearing Fault Diagnosis Model. IEEE Access 2023; 11: 51282-51295, doi: 10.1109/ACCESS.2023.3274696
16. Bórnea YP, Vitor ALO, Goedtel A, Castoldi MF, Souza WA, Barbara GV. A novel method for detecting bearing faults in induction motors using acoustic sensors and feature engineering. Appl Acoust 2025, 234, <https://doi.org/10.1016/j.apacoust.2025.110627>
17. Xu B, Li H, Ding R, Zhou F. Fault diagnosis in electric motors using multi-mode time series and ensemble transformers network. Sci Rep 2025, 15 7834, <https://doi.org/10.1038/s41598-025-89695-6>
18. Yang C, Cai B, Wu Q, Wang C, Ge W, Hu Z et al. Digital twin-driven fault diagnosis method for composite faults by combining virtual and real data. J of Ind Inf Integr 2023, 33, <https://doi.org/10.1016/j.jii.2023.100469>
19. Yang C, Cai B, Kong X, Zhang R, Gao C, Liu X et al. Fast and stable fault diagnosis method for composite fault of subsea production system. Mech Syst And Sign Proc 2025, 226, <https://doi.org/10.1016/j.ymsp.2025.112373>
20. Yang C, Cai B, Zhang R, Zou Z, Kong X, Shao X et al. Cross-validation enhanced digital twin driven fault diagnosis methodology for minor faults of subsea production control system. Mech Syst And Sign Proc 2023, 204, <https://doi.org/10.1016/j.ymsp.2023.110813>
21. Faysal A, Ngui WK, Lim MH, Leong MS. Noise Eliminated Ensemble Empirical Mode Decomposition Scalogram Analysis for Rotating

- Machinery Fault Diagnosis. *Sensors* 2021; 21(8) 8114, <https://doi.org/10.3390/s21238114>
22. Zhang J, Kong X, Cheng L, Qi H, Yu M. Intelligent fault diagnosis of rolling bearings based on continuous wavelet transform-multiscale feature fusion and improved channel attention mechanism. *Eksplloatacja i Niezawodność – Maintenance and Reliability* 2023; 25(1), <https://doi.org/10.17531/ein.2023.1.16>
 23. Chandra DG, Reddy US, Uma G, Umopathy M. Group normalization-based 2D-convolutional neural network for intelligent bearing fault diagnosis. *J Braz Soc Mech Sci Eng.* 2023; 45 584, <https://doi.org/10.1007/s40430-023-04491-5>
 24. Lu X, Xiao Y. Fault diagnosis method of automobile rolling bearing based on transfer learning and improved DenseNet. *Eksplloatacja i Niezawodność – Maintenance and Reliability* 2025; 25(2), <https://doi.org/10.17531/ein/194675>
 25. Gao Y, Li X. Fault Diagnosis of Centrifugal fan Bearings Based on I-CNN and JMMD in the Context of Sample Imbalance. *Eksplloatacja i Niezawodność – Maintenance and Reliability* 2024; 26(4), <https://doi.org/10.17531/ein/191459>
 26. Głowacz A, Sulowicz M, Zielonka J, Li Z, Głowacz W, Kumar A. Acoustic fault diagnosis of three-phase induction motors using smartphone and deep learning. *Exp Syst with Appl* 2025, 262, <https://doi.org/10.1016/j.eswa.2024.125633>
 27. Tang M, Liang L, Zheng H, Chen J, Chen D. Anomaly Detection of Permanent Magnet Synchronous Motor Based on Improved DWT-CNN Multi-Current Fusion. *Sensors* 2024; 24 2553, <https://doi.org/10.3390/s24082553>
 28. Chu KSK, Chew KW, Chang YC, Morris S. An Open-Circuit Fault Diagnosis System Based on Neural Networks in the Inverter of Three-Phase Permanent Magnet Synchronous Motor (PMSM). *World Electr Veh J.* 2024; 15(2), <https://doi.org/10.3390/wevj15020071>
 29. Ertargin M, Yildirim O, Orhan A. Mechanical and electrical faults detection in induction motor across multiple sensors with CNN-LSTM deep learning model. *Electr Eng.* 2024; <https://doi.org/10.1007/s00202-024-02420-w>
 30. Bharatheedasan K, Maity T, Kumaraswamidhas LA, Durairaj M. An intelligent of fault diagnosis and predicting remaining useful life of rolling bearings based on convolutional neural network with bidirectional LSTM. *Sādhanā* 2023; 48(131), <https://doi.org/10.1007/s12046-023-02169-1>
 31. Mohammad-Alikhani A, Nahid-Mobarakeh B, Hsieh M-F. One-Dimensional LSTM-Regulated Deep Residual Network for Data-Driven Fault Detection in Electric Machines. *IEEE Transactions on Industrial Electronics* 2024; 71(3): 3083-3092, doi: 10.1109/TIE.2023.3265054.
 32. Khawaja AU, Shaf A, Thobiani FA, Ali T, Irfan M, Pirzada AR et al. Optimizing Bearing Fault Detection: CNN-LSTM with Attentive TabNet for Electric Motor Systems. *Comput Model Eng Sci.* 2024; 141(3): 2399–2420, <https://doi.org/10.32604/cmescs.2024.054257>
 33. Tang S, Jiang Y, Su H, Zhu Y. A fault identification method of hydraulic pump fusing long short-term memory and synchronous compression wavelet transform. *Appl Acoust* 2025, 232, <https://doi.org/10.1016/j.apacoust.2025.110553>
 34. Li X, Su K, He Q, Wang X, Xie Z. Research on Fault Diagnosis of Highway Bi-LSTM Based on Attention Mechanism. *Eksplloatacja i Niezawodność – Maintenance and Reliability* 2023; 25(2), <https://doi.org/10.17531/ein/162937>
 35. Xu B, Li H, Liu Y, Zhou F, Yan B. Fault diagnosis in asynchronous motors based on an optimal deep bidirectional long short-term memory networks. *Meas Sci Technol.* 2023; 34(12), <https://doi.org/10.1088/1361-6501/acf681>
 36. Lale T, Yüsek G. Identification and classification of turn short-circuit and demagnetization failures in PMSM using LSTM and GRU methods. *Bulletin of the Polish Academy of Sciences Technical Sciences* 2025; 73(1), DOI: 10.24425/bpasts.2024.151958
 37. Yun E, Jeong M. Acoustic Feature Extraction and Classification Techniques for Anomaly Sound Detection in the Electronic Motor of Automotive EPS. *IEEE Access* 2024; 12: 149288-149307, doi: 10.1109/ACCESS.2024.3471169
 38. Samanta S, Bera JN, Biswas A. Induction Motor Inter-turn Short Circuit Fault Classification by Extracting Auto Features Using LSTM Neural Network. 2024 IEEE 3rd International Conference on Control, Instrumentation, Energy and Communication, CIEC 2024 – Proceedings 2024; 180-185, DOI: 10.1109/CIEC59440.2024.10468522
 39. Benbouzid MEH. A review of induction motors signature analysis as a medium for faults detection. *IEEE Transactions on Industrial Electronics* 2000; 47(5): 984-993, doi: 10.1109/41.873206
 40. Zeiler A, Faltermeier R, Keck IR, Tome AM, Puntonet CG, Lang EW. Empirical Mode Decomposition - an introduction. The 2010 International Joint Conference on Neural Networks (IJCNN) 2010; Barcelona, Spain, 1-8, doi: 10.1109/IJCNN.2010.5596829.
 41. Huang NE, Shen Z, Long SR, Wu MC, Shih HH, Zheng Q et al. The empirical mode decomposition and the Hilbert spectrum for nonlinear and non-stationary time series analysis. *Proceedings of the Royal Society A* 1998; 454: 903-995, <http://doi.org/10.1098/rspa.1998.0193>

42. Wharton AM, Sekar Iyengar AN, Janaki MS. Study of nonlinear oscillations in a glow discharge plasma using empirical mode decomposition and Hilbert Huang transform. *Phys. Plasmas* 2013; 20(2), 022301. <https://doi.org/10.1063/1.4789853>
43. Viney TJ, Sarkany B, Ozdemir AT, Hartwich K, Schweimer J, Bannerman D et al. Spread of pathological human Tau from neurons to oligodendrocytes and loss of high-firing pyramidal neurons in aging mice. *Cell Rep.* 2022; 41(7), doi: 10.1016/j.celrep.2022.111646
44. Zhang Q, Ma W, Li G, Ding J, Xie M. Fault diagnosis of power grid based on variational mode decomposition and convolutional neural network. *Electric Power Systems Research* 2022; 208 107871, <https://doi.org/10.1016/j.epr.2022.107871>.
45. Chen Y, Zhou C, Yuan J, Jin Z. Applications of empirical mode decomposition in random noise attenuation of seismic data. *Journal of Seismic exploration* 2014; 23: 481-495,
46. Song J-G, Zhao C-X, Lin S-H, Liu H-J. Decomposition of seismic signal based on Hilbert-Huang transform. 2011 International Conference on Business Management and Electronic Information 2011; Guangzhou, 813-816, doi: 10.1109/ICBMEI.2011.5917060
47. Goodfellow I, Bengio Y, Courville A. "Sequence Modeling: Recurrent and Recursive Nets" in *Deep Learning*, MIT Press, 2016, 404-411, [Online], <https://www.deeplearningbook.org/>, accessed February 2025
48. Olickal SJ, Jose R. LSTM projected layer neural network-based signal estimation and channel state estimator for OFDM wireless communication systems. *AIMS Electronics and Electrical Engineering* 2023; 7(2): 187-195, doi: 10.3934/electreng.2023011
49. Jia Y, Wu Z, Xu Y, Ke D, Su K. Long Short-Term Memory Projection Recurrent Neural Network Architectures for Piano's Continuous Note Recognition. *Journal of Robotics* 2017; 2017 2061827, 2017. <https://doi.org/10.1155/2017/2061827>